Proceedings of the
Annual Stability Conference
Structural Stability Research Council
Orlando, Florida, April 12-15, 2016

New Component-Based Model for Single-Plate Shear Connections with Pre-tension

Jonathan M. Weigand[1]

Abstract

Although simple shear connections are typically idealized as perfectly pinned, the actual resistance of the gravity framing system to flexural and axial loads can be critical in evaluating the robustness and stability of steel buildings subjected to extreme loads such as earthquakes, fire, and column loss. There are several key reasons for including more realistic connection behaviors in the design and analysis of steel buildings for extreme loads: (i) the gravity connections may develop large localized deformations under combined flexural and axial loading, potentially precipitating their failure (e.g. due to local buckling, fracture of the bolts, etc.), (ii) the gravity connections provide critical lateral bracing to the columns, and failure of connections could lead to global instability (potentially resulting in disproportionate collapse), and (iii) accurately accounting for contributions from the gravity system in design could effectively reduce the demands on the lateral load-resisting system, thus reducing costs. In order to include contributions from the steel gravity frames in structural analysis and design, validated and computationally efficient analysis tools are needed. This paper describes a component-based model for single-plate shear connections that includes the effects of pre-tension and accommodates both standard and slotted holes, accounting for deformations associated with bolt slip, bolt bearing, and bolt shear. The model also accounts for load reversals and pinching effects associated with hysteresis, thus providing the capability to model the connections under arbitrary in-plane load histories. Validation cases show that the model is capable of simulating connection response under both earthquake and column removal loading.

1. Introduction

Tests of steel gravity framing systems have shown that steel gravity connections contribute to the capacity and robustness of structural systems subjected to extreme loads such as earthquakes, fire, and column removal. However, in the design of structures for seismic and/or wind loads, contributions from the gravity connections to the lateral-load resisting system are often ignored (with the gravity connections idealized as perfectly pinned), even though gravity connections may comprise the majority of the steel framing connections. Tests of bare-steel single-plate shear connections under earthquake loads have demonstrated that the connections provide moment capacities on the order of 15 % to 20 % of their beam plastic moment capacities, and when composite with a concrete slab on steel deck, they provide capacities on the order of 30 % to 60 %

[1] Research Structural Engineer, National Institute of Standards and Technology (NIST), Gaithersburg, MD, jonathan.weigand@nist.gov

of their beam plastic moment capacities (Liu and Astaneh-Asl 1999). Including contributions from the steel gravity frames in capacity calculations of the lateral force resisting system during the design stage could be advantageous in the design and analysis of new structures, by reducing the cost of the overall structural system and making steel moment frame or braced frame buildings more competitive with concrete buildings. Even if the gravity connections are not included in the design of the lateral load resisting system, including their contributions in building analyses under amplified design loads (i.e., the Federal Emergency Management Agency (FEMA) P-695 methodology (FEMA 2009)) could provide a quantifiable measure of inherent robustness (or reserve capacity) in the structural system, a topic of widespread current interest in the structural engineering community. A recent study on 1-, 2-, 4-, and 8-story non-ductile steel moment framed buildings subjected to the FEMA P-695 "Far-Field" ground motion set showed that including gravity frames in the building analyses reduced the probability of collapse by 45 % (on average), when compared with analyses of the moment frames only (Judd and Charney 2014).

The role of the gravity connections in the system robustness is potentially even more critical when considering the response of steel buildings to column loss. Large-scale tests of steel gravity framing systems under column removal (Johnson et al. 2014; Johnson and Meissner 2015) have shown that the system robustness is largely dependent on the capacity of the connections to remain intact after undergoing highly-localized rotation and axial displacement demands. However, the results of full-scale tests of steel gravity connections under column removal demands available in the literature remain limited to just a handful of connection configurations and load histories. To evaluate general structural robustness, researchers and engineers need accurate and validated analysis tools to simulate the connection behavior over a wide range of connection configurations and under more general load histories.

Several researchers (e.g., Sadek et al. (2008), Wen et al. (2013b), Main and Sadek (2014), Weigand (2014)) have shown that detailed finite element models can accurately simulate the behavior of single-plate shear connections under earthquake loads and/or column removal scenarios, which are used to evaluate the potential for disproportionate collapse. However, the need to model large structural systems in engineering design practice makes detailed modeling of complete structural systems infeasible. Main and Sadek (2014) recognized these limitations, and used results from their detailed finite element models to calibrate a biaxial spring to represent each bolt row in a single-plate shear connection, with stiffness parameters estimated based on linear regression of rotational stiffness data from seismic testing. They showed that a reduced-order modeling approach provided good agreement with push-down tests of two-span beam assemblies by Thompson (2009).

Other researchers (e.g., Liu and Astaneh-Asl (2004), Foley et al. (2006), Wen et al. (2013a)) have used lumped plasticity springs as a simplified means to capture the connection moment-rotation and axial force-deformation behaviors. While lumped plasticity models do provide a fairly complete description of the connection backbone response under pure rotation or pure axial deformation, they cannot account for interactions between the connection flexural and axial behaviors. Thus, they may not be appropriate for design under extreme loads as: (i) during earthquakes, the gravity connections may be subjected to significant axial loads in addition to rotations (Astaneh-Asl 2005), and (ii) for column removal scenarios, the development of catenary action requires the connections to accommodate large axial deformations in combination with

large rotations (Sadek et al. (2008), Oosterhof and Driver (2012), Main and Sadek (2014), Weigand (2014)).

Component-based models provide a natural framework for capturing the complex behaviors of steel gravity connections under extreme loads as they including both fastener and connected element deformations, and provide automatic coupling between the in-plane flexural and axial behaviors. A number of component-based models are already available in the literature for certain types of steel gravity connections (e.g., bolted end-plate, bolted angle connections), but models for single-plate shear connections are relatively few. In addition to Main and Sadek (2014), described above, Elsati and Richard (1996) provided backbone response parameters for 76 mm (3.0 in) segments of single-plate shear connections and showed that component-based models could be used to model the connection pushover moment-rotation response. Weigand and Berman (2008) also used component-based models to determine the moment-rotation response of single-plate shear connections, but with the backbone response curve parameters taken from a model developed by Rex and Easterling (1996), and including multilinear hysteretic rules for the component unload/reload behaviors. Yu et al. (2009) likewise used the bolt-bearing curve developed by Rex and Easterling (1996) to model the backbone response of the connection segments, but with empirically modified stiffness values derived from finite element analysis results to model temperature dependence. Most recently, Koduru and Driver (2014) modified the empirical calibration factors determined by Yu et al. (2009), and also included shear yielding and shear fracture, to model the response of single-plate shear connections under column removal.

This paper summarizes a new component-based connection model for single-plate shear connections that includes the effects of pre-tension in the bolts and provides the capability to model connections with standard and slotted holes. The model is exercised under both cyclic rotations, representative of earthquakes, and combined rotations and axial deformations, representative of column removal scenarios. Results from these representative cases show that the model can be used to predict connection force and rotation/deformation capacities under both seismic loads and column removal scenarios.

2. Component-based Connection Model

In component-based connection models, the connection is notionally discretized into characteristic-width segments with aggregate force-displacement behaviors represented by discrete connection springs (Fig. 1a). Each characteristic-width segment captures contributions from the shear-plate, bolt, and beam-web, which are modeled as individual component springs in series as shown in Fig. 1(b) and Fig. 1(c)). The formulations for the backbone and hysteretic responses of the component springs are discussed in detail in the sections below.

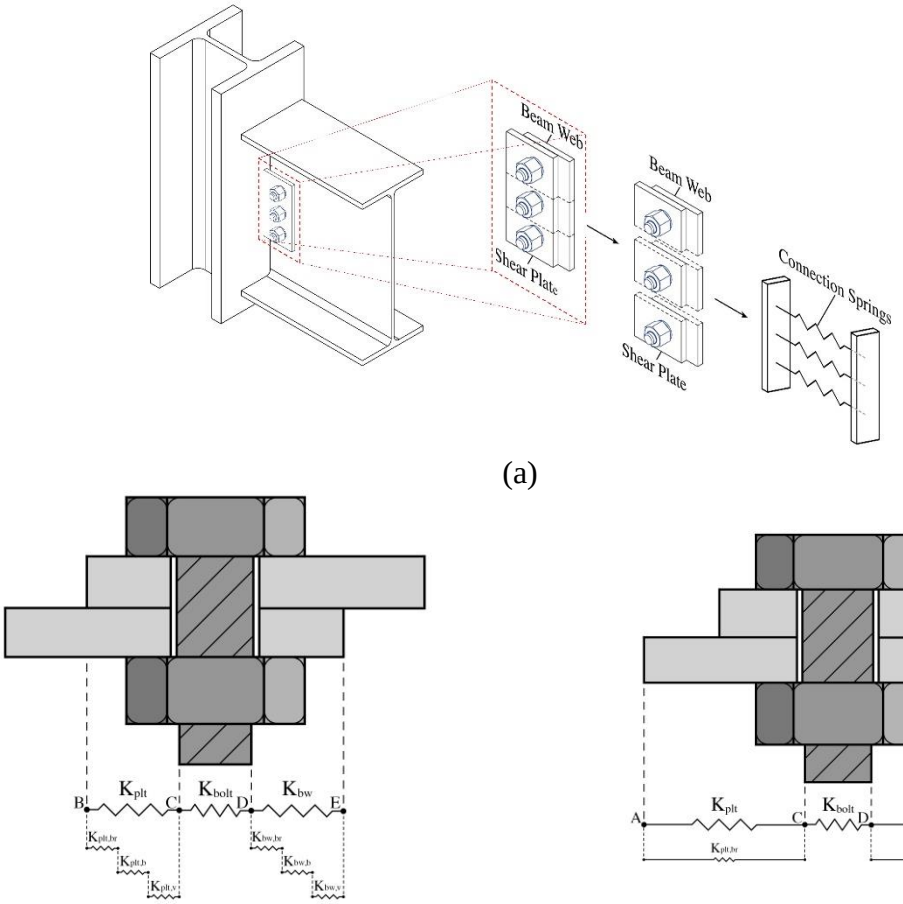

Figure 1: (a) Discretization of single-plate shear connection into connection springs, (b) connection spring stiffness contributions in tension, and (c) connection spring stiffness contributions in compression

2.1 Bolt Behavior

The transverse force-deformation behavior of the bolt, including shear and flexural effects, is modeled using Eq. (1) as:

$$R_{\text{bolt}} = R_{\text{unl}} + \frac{(K_{\text{i,bolt}} - K_{\text{p,bolt}})(\Delta_{\text{bolt}} - \Delta_{\text{unl}})}{\left(1 + \left|\frac{(K_{\text{i,bolt}} - K_{\text{p,bolt}})(\Delta_{\text{bolt}} - \Delta_{\text{unl}})}{R_{\text{cyc,bolt}}}\right|^{n_{\text{bolt}}}\right)^{(1/n_{\text{bolt}})}} + K_{\text{p,bolt}}(\Delta_{\text{bolt}} - \Delta_{\text{unl}}) \ , \qquad (1)$$

where Δ_{bolt} is the bolt shear deformation, R_{bolt} is the bolt shear force, $(\Delta_{\text{unl}}, R_{\text{unl}})$ are the coordinates of the last unload point, $R_{\text{cyc,bolt}} = \text{sign}(\Delta - \Delta_{\text{unl}})R_{\text{v,bolt}} - R_{\text{unl}} + K_{\text{p,bolt}}\,\Delta_{\text{unl}}$ is the cyclic reference load for the bolt shear force-deformation behavior where $R_{\text{v,bolt}} = 0.62F_{\text{u,bolt}}A_{\text{b}}$ (J3-1) is the shear capacity of the bolt, $n_{\text{bolt}} = 2$, A_{b} is the bolt cross-sectional area and $F_{\text{u,bolt}}$ is the tensile strength of the bolt material. Fig. 2(a) shows a comparison of the bolt backbone force-displacement response to data from three bolt-shear tests for 19 mm (3/4 in) diameter A325 bolts from Weigand (2014). Fig. 2(b) shows the behavior of the bolt under increasing magnitude cyclic shear deformations.

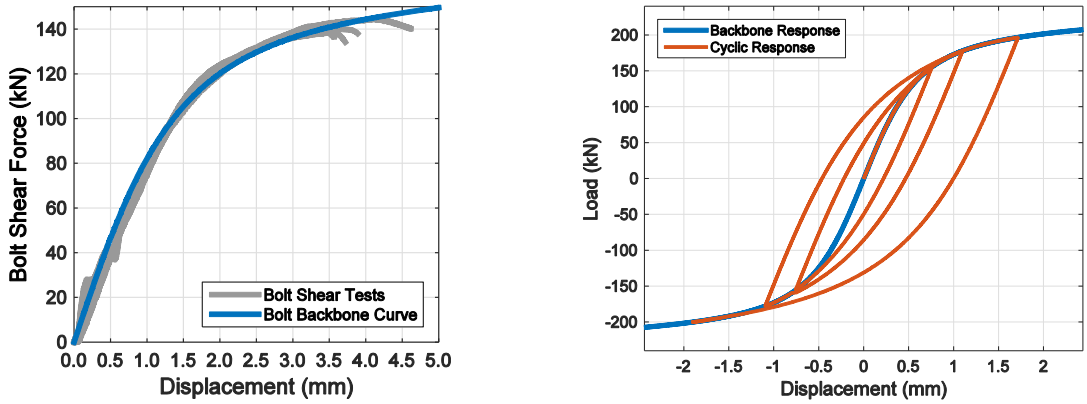

(a) (b)

Figure 2: (a) Comparison of bolt shear component spring backbone response with bolt shear data from Weigand (2014)[2], and (b) bolt shear component spring cyclic response

The initial stiffness of the bolt force-deformation response is calculated using the bolt bearing stiffness $K_{\mathrm{br,bolt}}$ and the bolt shearing stiffness $K_{\mathrm{v,bolt}}$ as

$$K_{\mathrm{i,bolt}} = \frac{1}{\frac{1}{K_{\mathrm{br,bolt}}} + \frac{1}{K_{\mathrm{v,bolt}}}} \quad . \tag{2}$$

The bearing stiffness is calculated as

$$K_{\mathrm{br,bolt}} = \frac{1}{1+3\beta_{\mathrm{b}}} \left(\frac{t_{\mathrm{p}} t_{\mathrm{w}} E_{\mathrm{bolt}}}{2(t_{\mathrm{p}}+t_{\mathrm{w}})} \right) , \tag{3}$$

based on the work by Nelson et al. (1983), where β_{b} is a correction factor that accounts for the concentration of bearing forces at the interface between plates for bolt in single shear. The value of β_{b} can range from 1 for a simple shear pin to relatively small values (on the order of 0.15) for pre-tensioned bolts with large bolt heads, washers, and nuts. For the analyses included in this paper, a value of $\beta_{\mathrm{b}} = 0.7$ was used. The bolt shearing stiffness is determined by assuming that the bolt acts as a prismatic Timoshenko beam with circular cross-section and fixed ends, such that:

$$K_{\mathrm{br,bolt}} = \frac{12 E_{\mathrm{bolt}} I_{\mathrm{bolt}}}{L_{\mathrm{bolt}}^3 (1+\Phi)} , \tag{4}$$

where E_{bolt} is the modulus of elasticity of the bolt, $I_{\mathrm{bolt}} = \pi d_b^2/64$ is the moment of inertia of the bolt shaft cross-section, $L_{\mathrm{bolt}} = t_{\mathrm{p}} + t_{\mathrm{w}}$ is the bolt length, and

$$\Phi = \frac{12 E_{\mathrm{bolt}} I_{\mathrm{bolt}}}{L_{\mathrm{bolt}}^2} \left(\frac{1}{\kappa G_{\mathrm{bolt}} A_{\mathrm{b}}} \right) \tag{5}$$

[2] Estimated uncertainty in measured experimental data less than 1 %

is a term in Timoshenko beam theory that characterizes the relative importance of the shear deformations to the bending deformations (Thomas et al. 1973). In Eq. (5), $G_{\text{bolt}} = E/2(1+\upsilon)$ is the bolt shear modulus, and κ is the shear coefficient for a circular cross-section, defined as:

$$\kappa = \frac{1}{\frac{7}{6}+\frac{1}{6}\left(\frac{\nu}{1+\nu}\right)} \ . \tag{6}$$

The bolt plastic shear stiffness, $K_{\text{p,bolt}}$, was assumed to be 2 % of the bolt initial shear stiffness, $K_{\text{i,bolt}}$.

2.2 Shear Plate and Beam Web Behavior

The shear-plate and beam-web component springs (i.e., plate springs) are modeled using a piecewise version the Richard Equation (see Richard and Abbott (1975)) such that:

$$R(\Delta) = \begin{cases} \dfrac{(K_{\text{b}}^{-}-K_{\text{p}}^{-})(\Delta-\Delta_{\text{br}}^{-})}{\left(1+\left|\dfrac{(K_{\text{b}}^{-}-K_{\text{p}}^{-})(\Delta-\Delta_{\text{br}}^{-})}{R_{\text{b}}^{-}}\right|^{n_{\text{b}}^{-}}\right)^{\left(1/n_{\text{b}}^{-}\right)}} + K_{\text{p}}^{-}(\Delta-\Delta_{\text{br}}^{-}), & \Delta \le \Delta_{\text{slipctr}} - \frac{1}{2}\Delta_{\text{slip}} \\ \dfrac{(K_{\text{i}}-K_{\text{y}})\Delta}{\left(1+\left|\dfrac{(K_{\text{i}}-K_{\text{y}})\Delta}{R_{\text{y}}}\right|^{n}\right)^{(1/n)}} + K_{\text{y}}\Delta, & \Delta_{\text{slipctr}} - \frac{1}{2}\Delta_{\text{slip}} \le \Delta \le \Delta_{\text{slipctr}} + \frac{1}{2}\Delta_{\text{slip}} \\ \dfrac{(K_{\text{b}}^{+}-K_{\text{p}}^{+})(\Delta-\Delta_{\text{br}}^{+})}{\left(1+\left|\dfrac{(K_{\text{b}}^{+}-K_{\text{p}}^{+})(\Delta-\Delta_{\text{br}}^{+})}{R_{\text{b}}^{+}(T)}\right|^{n_{\text{b}}^{+}}\right)^{\left(1/n_{\text{b}}^{+}\right)}} + K_{\text{p}}^{+}(\Delta-\Delta_{\text{br}}^{+}), & \Delta \ge \Delta_{\text{slipctr}} + \frac{1}{2}\Delta_{\text{slip}} \end{cases} \tag{7}$$

where the superscripts, $(\cdot)^{+}$ and $(\cdot)^{-}$, denote tensile and compressive deformations of the component spring, respectively, and the remaining parameters in Eq. (7) are defined below. Fig. 2(b) shows a schematic of the backbone response.

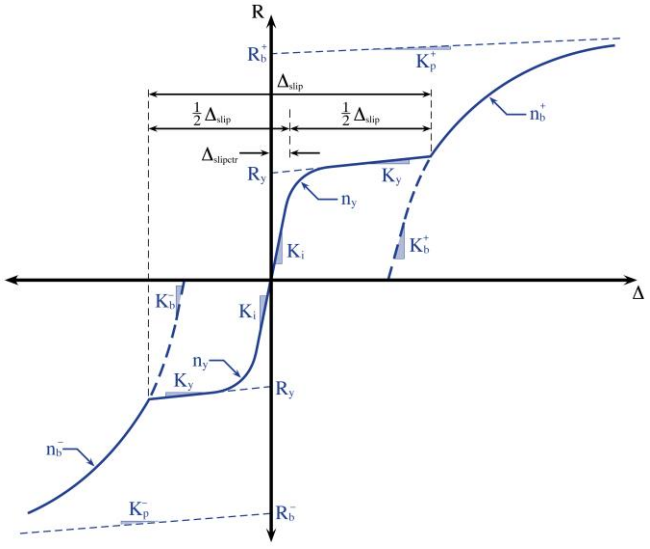

Figure 3: Plate component spring backbone force-displacement response

Prior to bearing, the single-plate shear connection resists load via friction due to the clamping force supplied by the bolt pre-tension and the surface contact between the bolt and plates. For slip-critical connections, the plates are assumed to behave elastically prior to slip, with initial stiffnesses determined from the gross areas of the plate characteristic-width segments as:

$$K_{\mathrm{i}} = \frac{w t_{\mathrm{p}} E}{a} \tag{8}$$

where w is the width of the shear plate segment, t_{p} is the plate thicknesses, E is the modulus of elasticity of the plate steel, and a is the distance between the column face to the bolt line. Connections that do not use pre-tensioned bolts may not develop the elastic plate stiffnesses, and thus may have significantly smaller initial stiffnesses. For connections without pre-tensioned bolts, the initial stiffness of the friction-slip behavior can be assumed to equal the initial plate bearing stiffness for the relevant loading direction, K_{b}^{+} or K_{b}^{-}, defined below.

Slip occurs as the loading overcomes the resistance supplied by the bolt pre-tension and friction between the sliding surfaces. After slip is initiated, the bolt continues to slip until the initiation of bearing contact between the bolt shaft and the bolt holes (at deformations of $\Delta_{\mathrm{slipctr}} - (1/2)\Delta_{\mathrm{slip}}$ in compression or $\Delta_{\mathrm{slipctr}} + (1/2)\Delta_{\mathrm{slip}}$ in tension, where Δ_{slip} is the difference between the plate hole diameter (or slot width, when applicable) and the bolt diameter).

The load at slip can be calculated as:

$$R_{\mathrm{slip}} = n_{\mathrm{f}} \mu \alpha A_b F_{\mathrm{u,bolt}} \ , \tag{9}$$

Where μ is coefficient of friction between the steel surfaces in contact, n_{f} is the number of faying surfaces (or slip planes), A_{b} and $F_{\mathrm{u,bolt}}$ were defined above, and α is the ratio of the bolt pre-tension load to the bolt tensile strength. For the modeling presented in this paper, $\alpha = 0.75$ was used and μ was taken as 0.338, corresponding to an average value calculated from a large set of data compiled by Grondin et al. (2007).

It should be noted that when connections are loaded dynamically, the load in the connection spring may decrease as the coefficient of friction decreases from the static to the kinetic coefficient of friction. However, most tests of single-plate shear connections, including those used for comparison with the model, have been conducted at sufficiently small loading rates that their behavior remained pseudo-static. For pre-tensioned bolts in pseudo-static tests, the resistance of the connection tends to remain relatively constant or even increase slightly as the bolts slip (e.g., Liu and Astaneh-Asl (2004), Weigand (2014)). While Eq. (7) allows for either positive or negative slip stiffnesses (designated as K_{y}), the comparison studies presented here found that a small positive value of 0.01 % of the initial stiffness was appropriate in all of the considered cases.

The capacity and stiffness parameters of bearing portion of the shear-plate and beam-web component behavior were adapted from the work of Rex and Easterling (1996), who performed 46 tests on a single bolt bearing against a single plate. The elastic and plastic bearing stiffnesses of the bearing force-deformation response can be determined from $K_{\mathrm{b}}^{+} = \beta_{\mathrm{s}} \overline{K}_{\mathrm{b}} \alpha_{K_{\mathrm{b}}}$ and $K_{\mathrm{p}}^{+} =$

$\beta_s \bar{K}_b \alpha_{K_p}$, where $\beta_s = 1$ for structural steel, $\alpha_{K_b} = 1.731$, and $\alpha_{K_p} = -0.009$ (see Rex and Easterling (1996)), and

$$\bar{K}_b = \frac{1}{\frac{1}{\bar{K}_b^{br}} + \frac{1}{\bar{K}_b^{b}} + \frac{1}{\bar{K}_b^{v}}} \tag{10}$$

with elastic stiffness contributions resulting from direct bearing ($\bar{K}_b^{br} = 120 t_p F_y d_b^{(4/5)}$), bending ($\bar{K}_b^{b} = 32 E t_p \left(L_{ehp} - d_b/2\right)^3$), and shearing ($\bar{K}_b^{v} = (20/3) G t_p \left(L_{ehp} - d_b/2\right)$). In the equations for the stiffness contributions, t_p is the plate thickness, d_b is the bolt diameter, F_y is the yield strength of the plate material, E is the modulus of elasticity of the plate material, and G is the shear modulus of the plate material.

The bearing response of the plates in compression is more constrained than that in tension, due to the additional restraint against bending provided by the plate welds. The additional constraint leads to a marginally stiffer force-deformation response in compression, relative to that in tension, an effect has also been noted experimentally for single-plate shear connections under increasing magnitude reversed cyclic loading (Crocker and Chambers 2004). The component spring bearing force-deformation response in compression mirrors the response in tension, but with initial elastic and plastic bearing stiffnesses based only on the direct bearing stiffness such that $K_b^- = \beta_s \bar{K}_b^{br} \alpha_{K_b}$ and $K_p^+ = \beta_s \bar{K}_b^{br} \alpha_{K_p}$. In compression, $\alpha_{K_p} = 0.001$ is taken as a small positive value to avoid the potential for a negative tangent stiffness.

Load Reversal Behavior

The behavior of single-plate shear connections upon load reversal can be relatively complex, but adequately capturing those complexities is critical to modeling the load-history-dependent resistance and energy dissipation capacity of the connections. Tests on single-plate shear connections under seismic loads have shown that the connection moment-rotation response becomes increasingly pinched and nonlinear at large rotations (e.g., Crocker and Chambers (2004), Liu and Astaneh-Asl (2004)). At small rotations prior to bearing, friction supplied by pre-tensioned bolts resists sliding in both directions, and the cyclic friction slip behavior at load reversal can be characterized by

$$R = R_{unl} + \frac{(K_i - K_y)(\Delta - \Delta_{unl})}{\left(1 + \left|\frac{(K_i - K_y)(\Delta - \Delta_{unl})}{R_{cyc}}\right|^{n_y}\right)^{(1/n_y)}} + K_y(\Delta - \Delta_{unl}) \ , \tag{11}$$

where, similar to the bolt shearing response, (Δ_{unl}, R_{unl}) are the coordinates of the last unload point and $R_{cyc} = \text{sign}(\Delta - \Delta_{unl}) R_y - R_{unl} + K_y \Delta_{unl}$ is the current value of the cyclic reference load. Eq. (11) represents a "full" (i.e., not pinched) cyclic hysteresis that is symmetric about the origin.

After bearing has been initiated, the plate component spring model also tracks the coordinates of the minimum and maximum unload points, $(\Delta_{unl,min}, R_{unl,min})$ and $(\Delta_{unl,max}, R_{unl,max})$ respectively. The load reversal behavior is then defined between the values of the minimum and

maximum unload points within the current cycle, permitting the model to capture the evolution of the connection response with increased hole elongations due to bearing. Pinching in the connection begins at the initiation of bearing deformations as a result of the loss of pre-tension in the bolts. This phenomenon is captured within the shear-plate and beam-web component springs by allowing the pinching (the scalar parameter γ in Eq. (15) below) to vary as a function of accumulated bearing deformation. The pinched hysteresis response is formed from a combination of two response curves. The first curve is the general form of the Richard Equation, which represents the response with no pinching, written in terms of the bearing curve parameters:

$$R = R_{\text{unl}} + \frac{(K_{\text{b}}^{+} - K_{\text{p}}^{+})(\Delta - \Delta_{\text{unl}})}{\left(1 + \left|\frac{(K_{\text{b}}^{+} - K_{\text{p}}^{+})(\Delta - \Delta_{\text{unl}})}{R_{\text{cyc}}}\right|^{n_{\text{b}}^{+}}\right)^{\left(1/n_{\text{b}}^{+}\right)}} + K_{\text{p}}^{+}(\Delta - \Delta_{\text{unl}}) \ , \tag{12}$$

where $R_{\text{cyc}} = R_{\text{b}}^{+} + R_{\text{y}}$ for the initial unload cycle, and $R_{\text{cyc}} = R_{\text{unl,max}} - R_{\text{unl,min}}$ for all subsequent cycles. The second curve, which represents the fully pinched response, is defined using a Bézier curve (e.g., Farin (1993), Prautizsch et al. (2002)). The Bézier curve was chosen because it provides an adaptable smoothly transitioning approximation to a piecewise-linear curve, that can be defined to traverse a path through zero load at zero displacement with a small residual stiffness K_{res}, and to terminate at the appropriate minimum or maximum unload point, depending on loading direction. The Bézier curve is calculated as

$$\boldsymbol{B}(t) = \sum_{i=0}^{n} B_i^n(t)\, \boldsymbol{P}_i \ , \tag{13}$$

where t is a parametric variable ranging from 0 to 1 (i.e., 0 at the current unload point and 1 at the current reload point),

$$B_i^n(t) = \binom{n}{i}(1-t)^{n-i}t^i \qquad i = 0, 1, \dots, n \tag{14}$$

are Bernstein polynomials, $\binom{n}{i} = \frac{n!}{i!(n-i)!}$ are the binomial coefficients, and $\boldsymbol{P}_i$ is the set of control points that define the curve trajectory (Fig. 4). Tests of connections under cyclic rotation cycles have shown that $K_{\text{rel}}^{-} \approx (1/2)K_{\text{b}}^{-}$ and $K_{\text{rel}}^{+} \approx (1/2)K_{\text{b}}^{+}$. At a given value of t, the Bézier curve resulting from Eq. (14) has two components, where the second component corresponds to the component spring load (i.e, $\boldsymbol{B}_2(t) = R_{\text{BZ}}$). R_{BZ} represents load reversal behavior that is fully pinched.

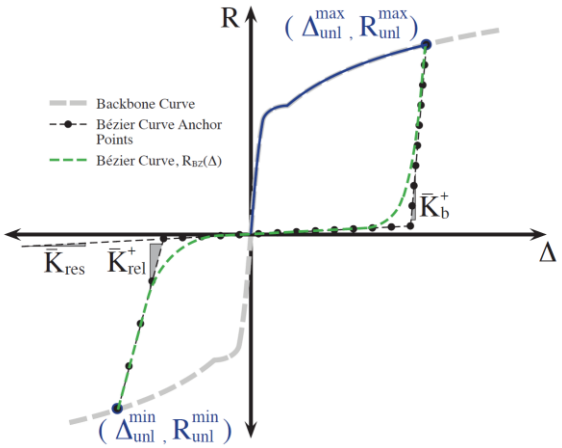

Figure 4: Schematic of Bézier curve with control points (unload from positive deformation)

The actual load reversal path R_p is calculated as a weighted summation between the full hysteretic behavior (i.e., Richard Equation) and fully pinched behavior (i.e., Bézier curve) as:

$$R_p = \gamma R + (1-\gamma) R_{BZ} \ , \tag{15}$$

where the amount that each curve contributes to the response defines the pinching ratio γ, which can vary between 0 and 1. Fig. 5(a) shows a schematic of the pinching behavior for the initial unload cycle and Fig. 5(b) shows a schematic of the pinching behavior for the subsequent cycles.

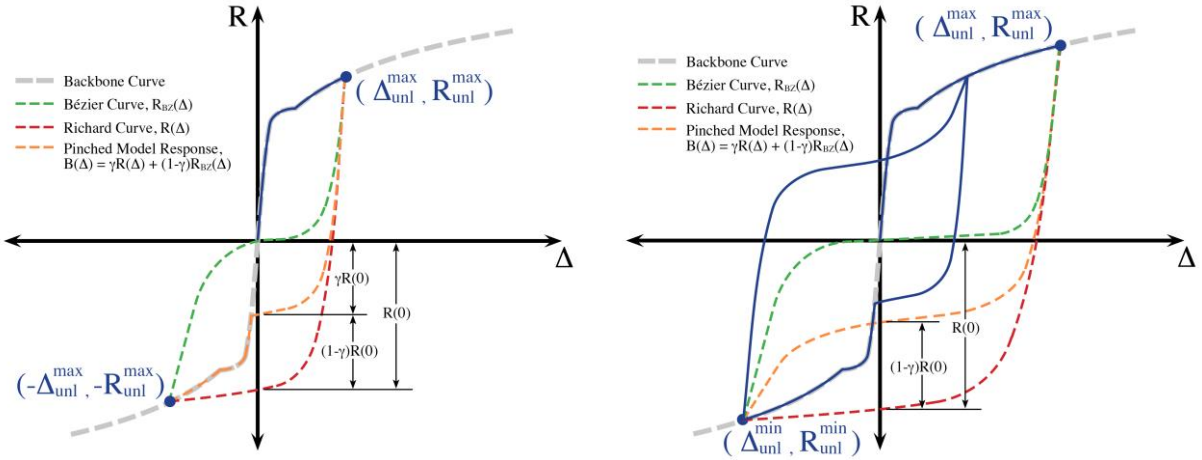

(a) (b)

Figure 5: Schematic showing plate component spring pinched hysteresis (Eq. (15)) for (a) initial unload cycle and (b) subsequent unload cycle

Calibration of Pinched Hysteresis

The evolution of the pinching parameter γ was determined by assuming that the bolt behaves elastically, and calibrating the shear-plate and beam-web component-spring pinching behavior against data from Liu and Astaneh-Asl (2004), for a four-bolt single-plate shear connection

subjected to increasing magnitude rotation cycles. The results of the pinching calibration are shown in Fig. 6(a), and Fig. 6(b) shows a comparison of the model response using the calibrated pinching function to the data from Liu and Astaneh-Asl (2004). More information on procedure used to calibrate the pinching parameter is available in Weigand (2016).

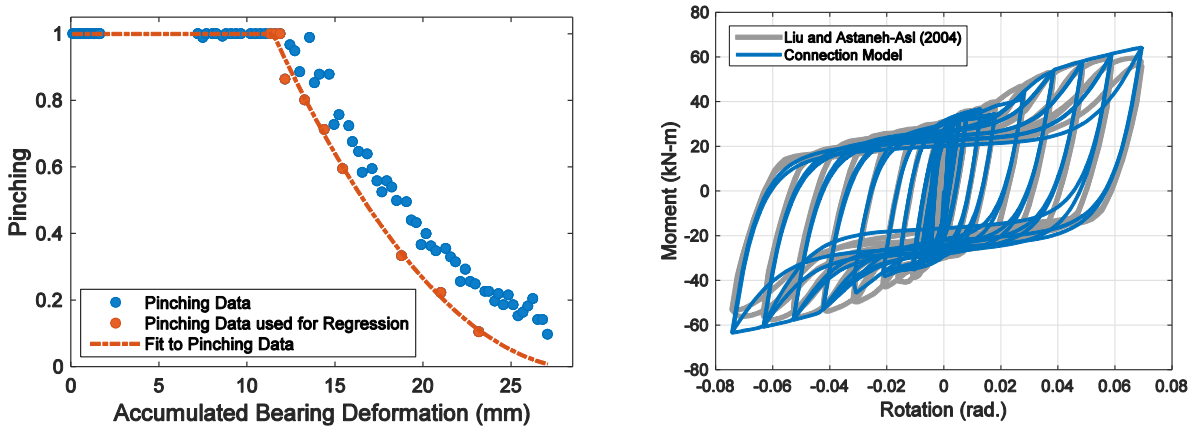

(a) (b)

Figure 6: (a) Pinching ratio data with fitted pinching curve, and (b) comparison of model response, using fitted pinching curve, to experimental data from Liu and Astaneh-Asl (2004)[3]

3. Calculation of Connection Deformations

The axial deformations of the connection springs, Δ_j, were calculated in terms of the connection rotation and axial deformation demands, θ and δ, respectively, using a rigid-body fiber-displacement model derived by Weigand and Berman (2014):

$$\Delta_j = \delta + (1 - \cos\theta)X_{j1} - \sin\theta X_{j2} \quad , \tag{16}$$

where $\boldsymbol{X}_j$ denotes the location of the j^{th} connection spring with components $\boldsymbol{X}_j = \{X_{j1}, X_{j2}\}^T$ relative to the center of rotation of the connection (Fig. 7). For seismic tests, the connections are subjected only to rotation demands (i.e., $\delta = 0$), and the connection spring deformations are essentially linear with increasing rotation.

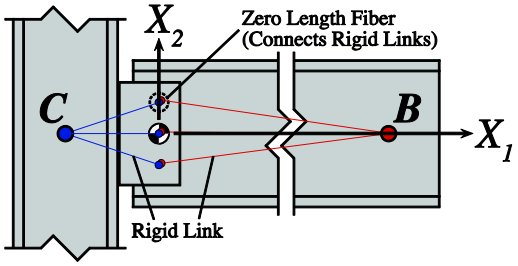

Figure 7: Coordinate system for calculation of spring displacements from rigid-body fiber displacement model (Source: Weigand and Berman (2014))

[3] Estimated uncertainty in measured experimental data less than 1 %

For the connections subjected to column loss, the connection demands can be calculated in terms of the vertical deflection of the simulated missing column, Δ_{syst}, (termed "simulated vertical displacement") as

$$\theta = \tan^{-1}\left(\frac{\Delta_{\text{syst}}}{L_{\text{r}}}\right) , \tag{17}$$

and

$$\delta = \frac{L_{\text{r}}}{2}\left[\sqrt{1+\left(\frac{\Delta_{\text{syst}}}{L_{\text{r}}}\right)^2} - 1\right] , \tag{18}$$

where L_{r} is the distance between the centers of gravity of connection bolt groups on the ends of the framing members (in the undeformed configuration).

4. Results and Discussion

To examine the ability of the component-based model to adequately capture the connection response, the model was used to predict the responses of multiple tested connections for which data are available in the literature. Fig. 8 shows a comparison of the predicted response from the model to the moments at the peak rotations from each cycle of data from Crocker and Chambers (2000), for a 4-bolt single-plate shear connection with 19 mm (3/4 in) diameter A325 bolts, a 9.5 mm (3/8 in) thick A36 shear plate, and a W18×55 beam section. It should be noted that, because Crocker and Chambers (2000) listed the material grades used in the connection tests, but did not include coupon data for the shear plate and beam web materials, this comparison assumed plate material yield and ultimate tensile strengths equal to the expected material strengths from ANSI/AISC 341-10 (AISC 2005). Fig. 8 shows that the model underestimated the resistance of the connection at small rotations, relative to the connection data, but better approximated the peak moments of the connection at large rotations. During the cycle prior to connection failure in the test, the model was within 5 % of the moments at the peak rotations (4 % at the cycle peak and 1 % at the cycle valley).

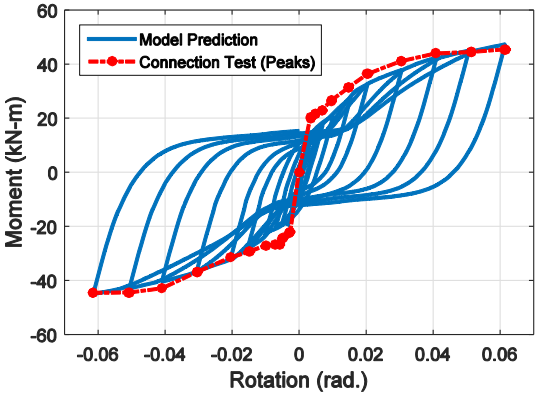

Figure 8: Comparison of moment-rotation response predicted by component-based model with connection data from Crocker and Chambers (2000)[4] (connection data shown at cycle peaks)

[4] Estimated uncertainty in measured experimental data less than 2 %

The component-based connection model was also compared to data from single-plate shear connection sub-assemblages tested by Weigand and Berman (2014) under simulated column removal. The model was subjected to the same rotation and axial deformation demands as were used in the sub-assemblage tests. The component spring displacements, due to the connection demands, were calculated from Eq. (16). Fig. 9 shows a comparison of the connection response predicted by the model with the vertical (i.e., along X_2) and horizontal (i.e., along X_1) force-displacement responses from Specimen sps4b|STD|34|38|48L from Weigand and Berman (2014), which corresponds to a 4-bolt single-plate shear connection with 19 mm (3/4 in) diameter bolts, a 9.5 mm (3/8 in) thick shear plate, and a 14.6 m (48 ft) span. The estimated uncertainty in the measured experimental data was less than ± 0.5 %, based on repeated calibrations of the instruments over the course of testing. The model under-predicts the connection vertical resistance throughout most of the analysis, relative to the connection data. This discrepancy occurs as a result of excess shear force in the tested connections, an effect which is described in detail in Weigand (2016). The model does not account for this excess shear force; however, as the excess shear force dissipates at large simulated vertical displacements (i.e., when the shear resistance of the connection is due primarily to tension resistance in the rotated configuration), the vertical force-displacement response of the model approaches that of the tested connection. The model predicted the peak vertical connection resistance within 4 % and the peak horizontal connection resistance within 1 %.

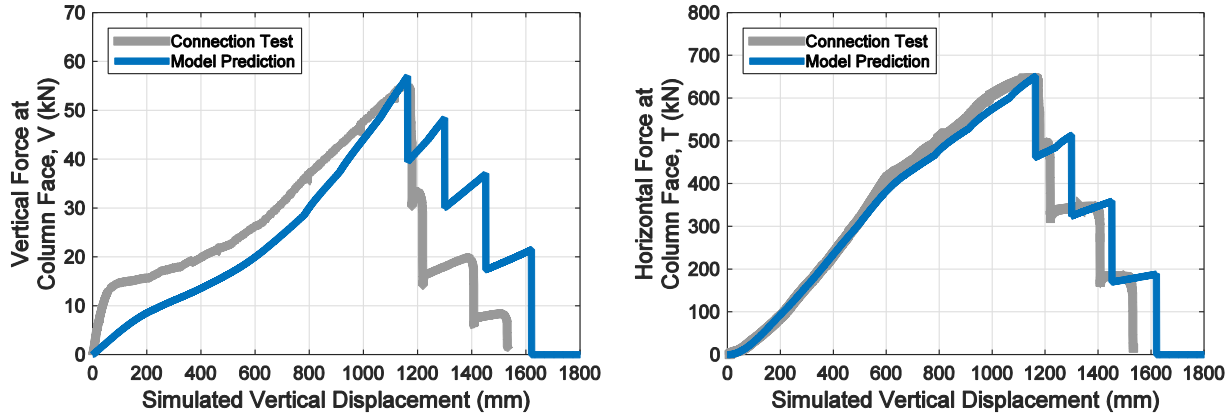

Figure 9: Comparison of predicted (a) vertical force-displacement response and (b) horizontal force-displacement response from component-based model with connection data

5. Summary

This paper summarized the development of a component-based model for single-plate shear connections. The model was compared against the moment-rotation response of a single-plate shear connection tested under increasing magnitude rotation cycles (i.e., seismic loads), as well as against the vertical and horizontal force-displacement responses of a connections tested under combined rotation and axial deformation demands (i.e., column removal loads). The close agreement between the model and the connection experiments, as well as additional comparisons between the model predictions and connection test data presented in Weigand (2016), serve as validation of the proposed modeling approach.

Beyond predicting the responses of the single-plate shear connection tests considered in this paper for validation, the component-based model provides other key capabilities, such as the capacity to capture load reversals and energy dissipation, that are critical to modeling the responses of connections subjected to extreme loads. The model also accounts for the pinching effects associated with hysteresis, which are critical to modeling the history-dependent resistance of connections under seismic loads, and which also play a role in the behavior of connections subjected to column removal.

Acknowledgments
Valuable comments on this work were provided by Dr. Joseph A. Main of the National Institute of Standards and Technology.

Disclaimer
Certain commercial entities, equipment, products, or materials are identified in this document in order to describe a procedure or concept adequately. Such identification is not intended to imply recommendation, endorsement, or implication that the entities, products, materials, or equipment are necessarily the best available for the purpose. Official contribution of the National Institute of Standards and Technology; not subject to copyright in the United States.

References
AISC (2005). *Seismic Provisions for Structural Steel Buildings*. American Institute of Steel Construction, Inc.

Astaneh-Asl, A. (2005). "Design of Shear Tab Connections for Gravity and Seismic Loads." University of California at Berkeley, Berkeley, CA.

Crocker, J. and Chambers, J. (2004). "Single plate shear connection response to rotation demands imposed by frames undergoing cyclic lateral displacements." *Journal of Structural Engineering*, 130(6), 934-941.

Elsati, M.K. and Richard, R.M. (1996). "Derived Moment Rotation Curves for Partially Restrained Connections." *Structural Engineering Review*, 8, 151-158.

Farin, G. (1993). *Curves and surfaces for computer aided geometric design. A practical guide.* Academic Press.

FEMA (2009). *Quantification of Building Seismic Performance Factors*. FEMA P695, Prepared by the Applied Technology Council for the Federal Emergency Management Agency, Washington, D.C.

Grondin, G., Jin, M., and Josi, G. (2007). "Slip critical bolted connections – a reliability analysis for design at the ultimate limit state." *Report No. Structural Engineering Report 274*, University of Alberta, Edmonton, Alberta.

Johnson, E.S. Meissner, and Fahnestock, L.A. (2015). "Experimental Behavior of a Half-Scale Steel Concrete Composite Floor System Subjected to Column Removal Scenarios." *Journal of Structural Engineering*, 04015133.

Johnson, E.S., Weigand, J.M., Francisco, T., Fahnestock, L.A., Liu, J., and Berman, J.W. (2014). "Large-Scale Experimental Evaluation of the Structural Integrity of a Composite Steel and Concrete Building Floor System." *ASCE/SEI Structures Congress*, Boston, MA.

Judd, J.P. and Charney, F.A. (2014). "Seismic Collapse Prevention Systems." *Tenth U.S. National Conference on Earthquake Engineering*, Anchorage, AK.

Koduru, S.D. and Driver, R.G. (2014). "Generalized component-based model for shear tab connections." *Journal of Structural Engineering*, 04013041.

Liu, J. and Astaneh-Asl, A. (1999). "Cyclic Testing of Simple Connections Including Slab Effects." Volume I: Results of Test Series "A", *Report No. UCB/CEE-Steel-99-01*, University of California at Berkeley, Berkeley, CA.

Liu, J. and Astaneh-Asl, A. (2004). "Moment-rotation parameters for composite shear tab connections." *Journal of Structural Engineering*, 130(9), 1371-1380.

Main, J. A. and Sadek, F. (2012). "Robustness of Steel Gravity Framing Systems with Single-Plate Shear Connections". Report Number NIST.TN.1749, U.S. Department of Commerce, National Institute of Standards and Technology.

Oosterhof, S.A. and Driver, R.G. (2012). "Performance of Steel Shear Connections under Combined Moment, Shear, and Tension." *ASCE/SEI Structures Congress*, Chicago, IL, 146-157.

Prautizsch, H., and Boehm, W., and Paluszny, M. (2002). *Bézier and B-Spline Techniques*. Springer Science & Business Media.

Rex, C.O. and Easterling, W.S. (1996). "Behavior and modeling of a single plate bearing on a single bolt." *Report No. CE/VP-ST 96/14*, Virginia Polytechnic Institute and State University, Blacksburg, VA.

Richard, R.M. and Abbott, B.J. (1975). "Versatile elastic-plastic stress-strain formulation". *Journal of the Engineering Mechanics*, 101(EM4), 511-515.

Sadek, F., El-Tawil, S., and Lew, H.S. (2008). "Robustness of Composite Floor Systems with Shear Connections: Modeling, Simulation, and Evaluation". *Journal of Structural Engineering*, 134(11), 1717- 1725.

Thomas, D.L., Wilson, J.M., and Wilson, R.R. (1973). "Timoshenko beam finite elements." *Journal of Sound and Vibration*, 31(3) 315-330.

Thompson, S.L. (2009). "Axial, shear, and moment interaction of single plate "shear tab connections." Ph.D. Dissertation in Civil Engineering, Milwaukee School of Engineering, Milwaukee, WI.

Weigand, J.M. (2014). "The Integrity of Steel Gravity Framing System Connections Subjected to Column Removal Loading." Ph.D. Dissertation in Civil Engineering, University of Washington, Seattle, WA.

Weigand, J.M. and Berman, J.W. (2008). "Rotation and strength demands for simple connections to support large vertical deflections." 14th *World Conference on Earthquake Engineering*, Beijing, China.

Weigand, J.M. and Berman, J.W. (2014). "Integrity of Steel Single Plate Shear Connections Subjected to Simulated Column Removal." *Journal of Structural Engineering*, 145 (5).

Weigand, J.M. (2016). "A Component-based Model for Single-Plate Shear Connections with Pre-tension and Pinched Hysteresis." *Journal of Structural Engineering*. In review.

Wen, R., Akbas, B., and Shen, J. (2013a). "Practical moment-rotation relations of steel shear tab connections." *Journal of Constructional Steel Research*, 88, 296-308.

Wen, R., Akbas, B., Sutchiewcharn, N., and Shen, J. (2013b). "Inelastic behaviors of steel shear tab connections." *The Structural Design of Tall and Special Buildings*, 23, 929-946.

Yu, H., Burgess, I.W., Davison, J.B., and Plank, R.J. (2009). "Experimental investigation of the behavior of fin plate connections in fire." *Journal of Constructional Steel Research*, 65, 723-736.